Simultaneous Deposition of W(VI) Species and Ni(II) Ions on the γ-Alumina Surface: Mechanistic Model

Nikos Spanos

Foundation of Research and Technology Hellas, Institute of Chemical Engineering and Chemical Processes at High Temperatures, P.O. Box 1414, GR-26500 Patras, Greece

Received: May 22, 1998; In Final Form: December 22, 1998

The simultaneous deposition (co-deposition) of W(VI) species and Ni(II) ions on the γ-alumina surface, from aqueous solutions using "equilibrium deposition followed by filtration" (EDF), has been studied in the pH range 4.2−6.2. It was found that the deposition of W(VI) species and Ni(II) ions on the γ-alumina surface in the presence of Ni(II) ions and W(VI) species, respectively, takes place mainly through adsorption of $W_xO_y^{z-}$ or Ni^{2+} ions on energetically equivalent sites at the inner Helmhotz plane (IHP), with strong attractive lateral interactions between the adsorbed ions. A mutual promotion in the deposition of W(VI) and Ni(II) species was observed at all pH values investigated. The protonated and deprotonated surface hydroxyls were found to be mainly responsible for the adsorption of the $W_xO_y^{z-}$ and Ni^{2+} ions, respectively, thus resulting in a decrease [increase] of the adsorbed amount of W(VI) species (Ni(II) ions) with increasing pH. Moreover, it was found that the presence of Ni(II) ions minimized the contribution of the neutral surface hydroxyls to the total W(VI) deposition. Finally, a model developed to describe the simultaneous deposition of W(VI) species and Ni(II) ions on the γ-alumina surface showed that as pH increased from 4.2 to 6.2 the deposition of W(VI) through adsorption of WO_4^{2-} ions increased at the expense of deposition of W(VI) through adsorption of $HW_6O_{20}(OH)_2^{5-}$ ions, which decreased.

Introduction

The classical methods of preparation of supported catalysts, that is, the dry (incipient wetness) or wet impregnation followed by drying, calcination, and/or activation, usually result in low dispersity of the supported phase. To overcome the problems associated with this method, the "equilibrium deposition followed by filtration (EDF)" technique, which results in relatively high dispersity, has been developed in the last few years.[1−24] Despite the high dispersity achieved by the EDF technique, the total amount of the supported phase and thus of the active surface obtained is not always sufficiently high because the concentration of the deposition sites is often low, depending on the impregnating parameters. Recent studies dealing with the mechanism of deposition, from aqueous solutions, of catalytically active species on the surfaces of γ-Al_2O_3 and TiO_2 revealed that these sites may be created by protonated [OH_2^+] or neutral [OH] surface hydroxyls for negative species (e.g., MoO_4^{2-}, WO_4^{2-}, CrO_4^{2-}) and by deprotonated surface hydroxyls [O^-] for positive ions (e.g., Co^{2+}, Ni^{2+}).[1,7,16,21−23,25−35] A number of studies have been devoted to the regulation of the concentration of the various types of surface groups of oxidic supports.[36−42] It was found that by changing the pH and temperature of the impregnating solution and doping the carrier with various amounts of dopants (Li^+, Na^+, F^-) it is possible to maximize the concentration of the deposition sites and thus the amount of the active species deposited by EDF. Unfortunately, in some cases the amount of the active species deposited by EDF is not sufficiently large even though the concentration of deposition sites has been maximized. This is, for instance, the case for the deposition of Co^{2+} and Ni^{2+} on the surface of γ-Al_2O_3.[31] This disadvantage may be overcome by simultaneously depositing one active species with another oppositely charged species because of the synergism between such ions.

In the present paper the simultaneous deposition (co-deposition) of the W(VI) species and Ni(II) ions on γ-alumina using EDF was investigated. This system was chosen to be studied because of the profound importance of the supported Ni−W/γ-Al_2O_3 catalysts in the hydrotreatment processes.

Despite the fact that some work concerning the mechanism of deposition of W(VI) species on γ-Al_2O_3 and of Ni(II) ions on the same substrate has been done,[24,31−33,43−46] reports on the W(VI) and Ni(II) co-deposition on γ-Al_2O_3 are very rare. The main purpose of this study was to investigate the role of the presence of Ni(II) ions in the impregnating solution, and consequently on the γ-alumina surface, on the uptake and the type (monomeric or polymeric) of the deposited W(VI) species. This feature is very important in the preparation of W−Ni/γ-alumina catalysts, because according to reports in the relevant literature, the catalytic activity strongly depends on the kind of the W(VI) species present.

Experimental Section

Materials. The support used in the present study was obtained by crushing Houdry Ho 415 γ-alumina extrudates [S_{BET} = 123 $m^2\ g^{-1}$, water pore volume = 0.45 $cm^3\ g^{-1}$]. After sieving, a fraction between 100 and 150 mesh was selected, impregnated with bidistilled water, dried at 120 °C for 2.5 h, and calcined at 600 °C for 12 h.

Crystalline ammonium tungstate ($(NH_4)_{10}W_{12}O_{41}5H_2O$), obtained from Ventron (99.999%), and the nickel nitrate ($Ni(NO_3)_2 6H_2O$), obtained from Fluka (98%), were, respectively,

10.1021/jp982341t CCC: $18.00
Published on Web 02/25/1999

used for the preparation of the tungstate and nickel aqueous stock solutions used in the deposition experiments as well as in the potentiometric titrations and microelectrophoretic mobility measurements. Crystalline ammonium nitrate (Riedel de Haen (99%)) was used for the preparation of the aqueous solutions of the background electrolyte employed in the potentiometric titrations and microelectrophoretic mobility measurements as well as for regulating the ionic strength of the tungstate and nickel solutions used in the deposition experiments. All solutions were filtered through membrane filters (Millipore) and were standardized by atomic absorption spectrometry (AAS Perkin-Elmer 305A) and ion chromatography (Metrohm IC 690).

Equilibrium Deposition Filtration (EDF). Equilibrium deposition experiments were done at 25.0 ± 0.1 °C and over a pH range between 4.2 and 6.2. This pH range was selected due to the increased solubility of γ-Al_2O_3 at pH values below 4.0[16] and the insolubility of nickel hydroxide at relatively high pH values.[47] Moreover, the increased solubility of alumina in the presence of the Ni^{2+} or Co^{2+} ions at neutral or basic impregnating solutions, observed by de la Caillerie et al.,[48] does not take place in the acidic pH range (4.2−6.2). The ionic strength, adjusted by ammonium nitrate, was 0.15 M, and the suspension pH was adjusted by adding small aliquots of standard strong acid or strong base solutions as needed. In each experiment a volume of 0.014 L of W(VI) and Ni(II) solutions containing over a range of concentrations was placed in small polyethylene vials and thermostated in a double walled, water-jacketed vessel at 25.0 ± 0.1 °C. The concentrations of both species were gradually increased from 1×10^{-3} to 2×10^{-2} mol L^{-1}, keeping their relative (molar) ratio constant. In a second series of deposition experiments, the concentration of one species was gradually increased from 1×10^{-3} to 2×10^{-2} mol L^{-1} whereas the concentration of the other species was kept constant. The solution pH was adjusted to a value close to the desired final pH value. pH measurements were done by a combination glass/(Ag−AgCl) electrode (Metrohm) standardized before and after each series of pH measurements with NBS standard buffer solutions. A precisely weighed mass of the support corresponding to a total surface area of about 5 m^2 was suspended in the solution, and the suspension was allowed to equilibrate with magnetic stirring. After 2 h of equilibration the suspension pH was readjusted to the desired final pH value, and the suspension was allowed to equilibrate for 20 h. Following equilibration, the pH was measured again, and the suspension was filtered through membrane filters (Millipore, 0.22 μm). The filtrate was analyzed spectrophotometrically for total tungsten (W_t)[49] and nickel (Ni_t).[50] The solid was characterized by X-ray fluorescence (XRF, GTN Spectrace). In each series of deposition experiments a blank was included to make sure that no tungstate and nickel species were deposited on the membrane filters or on the walls of the vials used for the deposition experiments.

The surface concentrations (mol m^{-2}) of the W(VI), Γ_W, and of the Ni(II), Γ_N, were determined from the difference in the concentration (mol L^{-1}) in the impregnating solution of W(VI) and Ni(II), before ($C_{o,W}$ and $C_{o,N}$) and after ($C_{eq,W}$, $C_{eq,N}$) deposition.

The above procedure was also followed in the equilibrium deposition experiments performed at 25.0 ± 0.1 °C and at pH 5.7 for the deposition of the W(VI) species in the absence of Ni(II) ions and at pH 5.1 for the deposition of the Ni(II) ions in the absence of W(VI) species. It should be noted that preliminary experiments showed that the deposition reached equilibrium after 2−4 h. Past this time period, the deposited amount of the W(VI) species as well as of the Ni(II) ions remained constant.

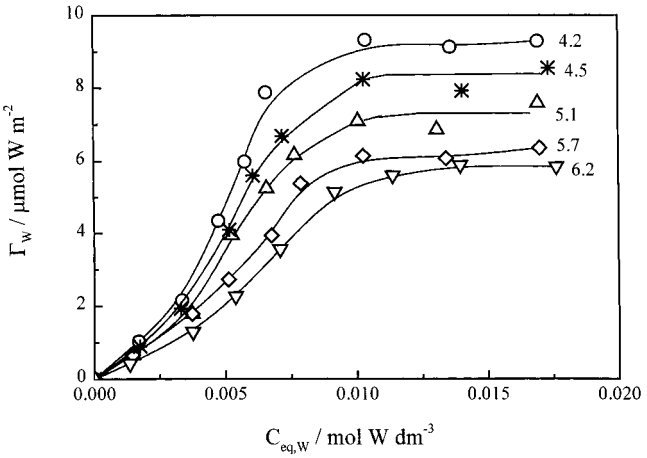

Figure 1. Uptake of W(VI) obtained during the co-deposition of W(VI) species and Ni(II) ions as a function of the equilibrium W(VI) concentration at various pH values. $T = 25$ °C, $I = 0.15$ mol L^{-1} NH_4NO_3. pH values are indicated.

Microelectrophoresis. The electrophoretic mobilities of the γ-alumina particles were measured in 0.01 mol dm^{-3} ammonium nitrate solutions at 25 ± 0.5 °C as a function of pH with a laser-Doppler velocimetric device (Zetasizer 5000, Malvern Instruments Ltd., Worcestershire, Great Britain) with an applied field strength of ca. 80 V cm^{-1}. Prior to the mobility measurement, the suspension was sonicated for 10 min. This time was determined to be needed for complete disaggregation of the suspensions. The particle size was also measured with the same instrument, and a mean value equal to 871 ± 135 nm was found. The velocity of the particles was measured at a certain depth of the cell where solvent is at rest (stationary level). The concentration of the suspension was adjusted within the operational limits of the instrument, and the suspension pH was adjusted by the addition of standard solutions of hydrochloric acid or potassium hydroxide (Merck, titrisol). The suspension pH value was measured before and after the mobility measurements. The reported electrophoretic mobilities are the averages of at least 10 sets of measurements (spread of values is ±10% of the reported mean values).

Potentiometric Titrations. The experimental procedure concerning the potentiometric titrations of electrolyte solutions or suspensions has been described in detail elsewhere.[27,37−40] According to this technique, the electrolyte solution or suspension is titrated using an acid, and the pH is recorded every 3 min as a function of the volume of titrant added. The above technique (fast titration) allows for the determination of the amount of the hydrogen ions consumed on the surface of the oxidic support (H_c^+). Details on this determination have been reported elsewhere.[30,31]

Results and Discussion

Semiquantitative Approach. An analysis of the results obtained from equilibrium deposition experiments, potentiometric titrations, and microelectrophoretic mobility measurements, without taking into account the kind of the deposited W(VI) species and the stoichiometry between deposition sites and deposited species, is first undertaken. The widely accepted triple-layer model for the electrical double layer (edl) was adopted in the present study.

Figures 1 and 2 illustrate the isotherms for W(VI) species' and Ni(II) ions' uptake obtained during their co-deposition at

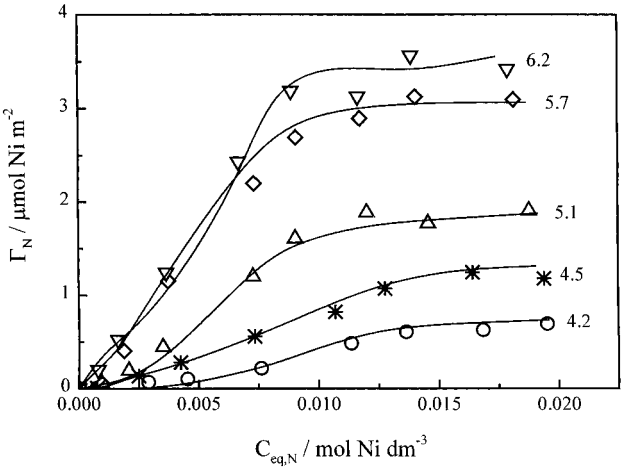

Figure 2. Ni(II) uptake obtained during the co-deposition of W(VI) species and Ni(II) ions as a function of the equilibrium Ni(II) concentration at various pH values. The solid lines represent the model calculations. $T = 25$ °C, $I = 0.15$ mol L^{-1} NH_4NO_3. pH values are indicated.

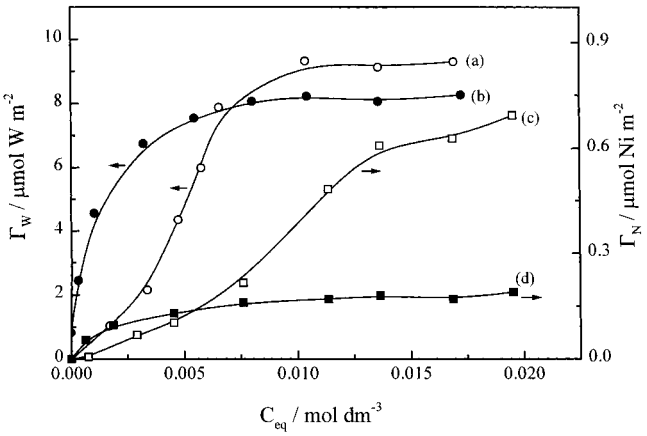

Figure 3. W(VI) (curves a, b) and Ni(II) (curves c, d) uptake obtained in the presence (curves a and c) and absence (curves b and d) of Ni(II) ions and W(VI) species, respectively, as a function of the equilibrium W(VI) and Ni(II) concentration, respectively. $T = 25$ °C, $I = 0.15$ mol L^{-1} NH_4NO_3, pH = 4.2. Curves (b) and (d) have been obtained from refs 32 and 31, respectively.

different pH values. Comparing these isotherms with those obtained for the deposition of W(VI) species in the absence of Ni(II) ions,[32] and for the deposition of Ni(II) ions in the absence of W(VI) species,[31] two important features may be observed. The first is the type of the obtained isotherms,which is S-type in the co-deposition and L-type in the separate deposition of W(VI) species and Ni(II) ions. The second is the fact that the saturation surface concentration, Γ_m, corresponding to the plateau of the respective isotherms, obtained for the W(VI) species (Ni(II) ions) in the presence of Ni(II) ions (W(VI) species) is slightly higher (much higher) than that obtained for the W(VI) species[32] (Ni(II) ions[31]) in the absence of Ni(II) ions (W(VI) species). A typical example of the mutual promotion in the deposition of W(VI) and Ni(II) species taking place during the co-deposition of these species is shown in Figure 3.

It is suggested that the L-type isotherms imply localized, Langmuir type adsorption at energetically equivalent sites located at the inner Helmholtz plane (IHP) of the electrical double layer (edl). The lateral interactions between the adsorbed species are negligible in comparison with the interactions

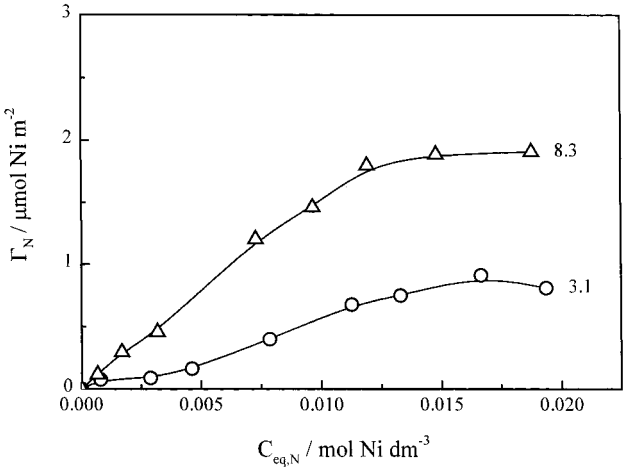

Figure 4. Isotherms for the Ni(II) deposition corresponding to different W(VI) uptakes (Γ_W/μmol W m^{-2}), obtained at pH = 5.1. $T = 25$ °C, $I = 0.15$ mol L^{-1} NH_4NO_3. Γ_W values are indicated.

between the adsorbed species and the substrate. Consequently, the activation energy of desorption is independent of the coverage of the support surface by the adsorbed species.[51,52] Concerning the S-type isotherms: they demonstrate a deviation from the Langmuir type behavior due to strong lateral interactions between the adsorbed species as compared with the respective interactions between the adsorbed species and the substrate, resulting in an increase in the activation energy of desorption with an increase in the coverage of the support surface by the adsorbed species.[51,52] It is therefore evident that the W(VI) species and Ni(II) ions deposited during their co-deposition are located at energetically equivalent sites at the IHP with lateral interactions which are stronger than those exerted between the W(VI) species[32] (Ni(II) ions[31]) deposited in the absence of Ni(II) ions (W(VI) species). It should be noted here that the speciation of the W(VI) species and Ni(II) ions in solution, done using the speciation software SURFEQL,[53] showed that in our experimental conditions (pH in the range 4.2−6.2, total tungsten and nickel concentration between (1×10^{-3}) and (2×10^{-2}) mol L^{-1}) all of the W(VI) is present in the form of negatively charged tungstate ions ($H_xW_yO_z(OH)_m^{n-}$) while nickel is present mainly as free Ni^{2+} ions, and the concentration of nickel hydroxo or ammonia complexes is negligible.[47] Thus, the stronger lateral interactions are electrostatic attractions exerted between the deposited anionic species of W(VI) and the cations of Ni(II), resulting in the already-mentioned mutual promotion of the deposition for the $W_xO_y^{z-}$ and Ni^{2+} ions caused by the Ni^{2+} and $W_xO_y^{z-}$ ions, respectively.

To study the effect of the deposited amount of W(VI) species or Ni(II) ions on the promotion of the deposition of the Ni(II) ions or W(VI) species, respectively, isotherms for the W(VI) species' or Ni(II) ions' uptake corresponding to a constant nickel or tungsten uptake were obtained at constant pH values. In Figure 4 it may be observed that the promotion of the deposition of the Ni(II) ions on the γ-alumina surface, caused by the co-deposited W(VI) species, increased with the amount of the co-deposited tungsten. A similar trend is not evident in the case of W(VI) species because the promotion of the tungsten deposition, caused by the co-deposited Ni(II) ions, is relatively low (compare curve a with curve b and curve c with curve d of Figure 3).

The mutual promotion in deposition of $W_xO_y^{z-}$ and Ni^{2+} ions during their co-deposition may also be inferred from the XRF spectra shown in Figure 5, for the samples NiO/γ-Al_2O_3

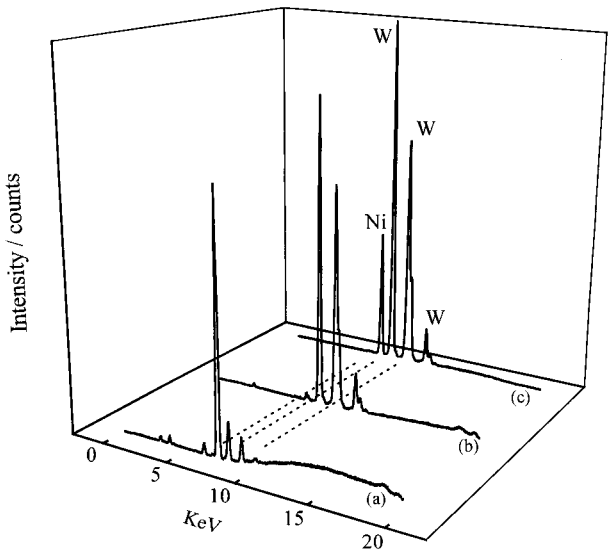

Figure 5. XRF spectra of the samples NiO/γ-Al_2O_3 (spectrum a), WO_3/γ-Al_2O_3 (spectrum b) and NiO−WO_3/γ-Al_2O_3 (spectrum c). The samples have been prepared using the EDF method at pH = 4.5 and T = 25 °C. I = 0.15 mol L^{-3} NH_4NO_3.

(spectrum a), WO_3/γ-Al_2O_3 (spectrum b), and WO_3−NiO/γ-Al_2O_3 (spectrum c), which have been prepared by using the EDF method. It may be observed that in spectrum c the intensity of the peaks corresponding to both nickel and tungsten are higher than the corresponding ones of spectra a and b.

As may be seen in Figure 1 (Figure 2), the tungsten uptake ($\Gamma_{W,m}$) (nickel uptake ($\Gamma_{N,m}$)) decreases (increases) with pH; i.e., it follows the same trend with the protonated ($AlOH_2^+$) (deprotonated (AlO^-)) surface hydroxyls. This trend shows that, in addition to the amount of the co-deposited ions, surface hydroxyls play an important role in the deposition of $W_xO_y^{z-}$ or Ni^{2+} ions on the surface of γ-alumina. Previous studies on the deposition of $W_xO_y^{z-}$ ions on the γ-alumina surface in the absence of Ni(II) ions showed that, in addition to the protonated surface hydroxyls, the undissociated groups contribute to the deposition of the $W_xO_y^{z-}$ ions.[32,46]. The participation of the undissociated groups to the deposition of $W_xO_y^{z-}$ ions in the presence of Ni(II) ions will be tested in the co-deposition model which will be described below.

As already mentioned, the S-type isotherms illustrated in Figures 1 and 2 suggest that the deposited $W_xO_y^{z-}$ and Ni^{2+} ions are located at the IHP. Additional information concerning the plane of the double layer where the deposited $W_xO_y^{z-}$ and Ni^{2+} ions are located could be obtained from the values of ζ-potential (the potential at the shear plane of the edl) determined in the presence of these ions, which are shown in Figure 6 (□). It should be noted here that the isoelectric point (iep) of γ-alumina impregnated in 0.01 mol L^{-1} NH_4NO_3 solution, i.e., in the absence of W(VI) species and Ni(II) ions, has been found to be at about pH 8.0.[27] The shift of the positive ζ-potential values, obtained at pH < 8.0 in the absence of $W_xO_y^{z-}$ and Ni^{2+} ions, to negative values, obtained in the presence of these ions (Figure 6), is characteristic of superequivalent adsorption of anions taking place at the IHP.[54] This suggestion is substantiated by the fact that the amount of the deposited $W_xO_y^{z-}$ ions is significantly larger than the amount of the deposited Ni^{2+} ions (cf. Figures 1 and 2), and thus, the location of these ions at the IHP should overcompensate for the positive surface charge and thus shift the positive ζ-potential, obtained in the absence of these ions at pH < 8.0, to negative values.

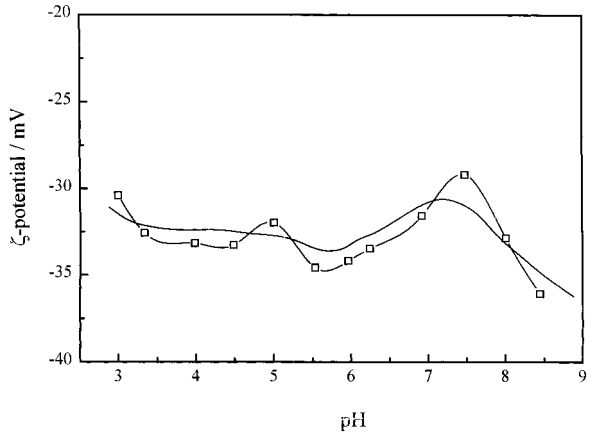

Figure 6. Variation of the ζ-potential, with pH, in the presence of $W_xO_y^{z-}$ (1×10^{-3} mol W^{VI} L^{-1}) and Ni^{2+} (1×10^{-4} mol Ni^{2+} L^{-1}) ions: (□) experimental values, (solid line) calculated values. T = 25 °C, I = 0.01 mol L^{-1} NH_4NO_3.

The location of the deposited Ni(II) ions at the IHP may also be investigated by mathematically analyzing the corresponding isotherms obtained for the uptake of Ni(II) ions. This analysis was done by deriving and testing two equations, assuming that the deposited ions are located first in the diffuse part of the double layer and second on the surface of the solid. The speciation calculations for nickel, in our experimental conditions, showed that all of the nickel is present as free Ni^{2+} ions. The analysis of the deposition isotherms was consequently done considering only the presence of free Ni^{2+} ions. A similar analysis of the deposition isotherms for W(VI) species was not possible because more than one W(VI) species is present in the solution.

Location of the Ni^{2+} Ions on the Surface. An equation describing the location of the deposited Ni^{2+} ions on the surface of γ-alumina may easily be derived by adopting a procedure reported earlier.[31] The surface excess of nickel ions, Γ_N, as a function of the equilibrium concentration of Ni(II) in solution, $C_{eq,N}$, may be described by eq 1

$$\ln \Gamma_N + (4F^2/RT\alpha)\Gamma_N = \ln \Gamma_{N,m} + (4F^2/RT\alpha)\Gamma_{N,m} + \ln C_{eq,N} \quad (1)$$

where F is the Faraday constant, R and T are the gas constant and the absolute temperature, respectively, and α is the total capacity of the electrical double layer (μF m^{-2}). Equation 1 may be written as

$$Y = A + BX \quad (2)$$

where $Y = \ln \Gamma_N + (4F^2/RT\alpha)\Gamma_N$, $A = \ln \Gamma_{N,m} + (4F^2/RT\alpha)\Gamma_{N,m}$, $B = 1$, and $X = \ln C_{eq,N}$. According to eq 2, a linear dependence of Y on X is predicted with slope equal to unity. A linear fit of the data was obtained for a value of the capacity equal to 7.6 $\times$ 10^5 F m^{-2} which is unrealistically higher than the values anticipated for oxides. It is, therefore, evident that eq 2 failed to fit the adsorption data, corroborating the qualitative finding that the Ni^{2+} ions are not located on the alumina surface.

Location of the Ni^{2+} Ions in the Diffuse Part of the Double Layer. Assuming that the Ni(II) ions taken up by the oxide surface are located in the diffuse part of the electrical double layer, the uptake may be described by eq 3[31]

$$\Gamma_N = \{(\epsilon\epsilon_0 kTN/2F^2)[\exp(-2e_0 y_d/kT) + 2\exp(e_0 y_d/kT) - 3]\}^{1/2} C_{eq,N}^{1/2} \quad (3)$$

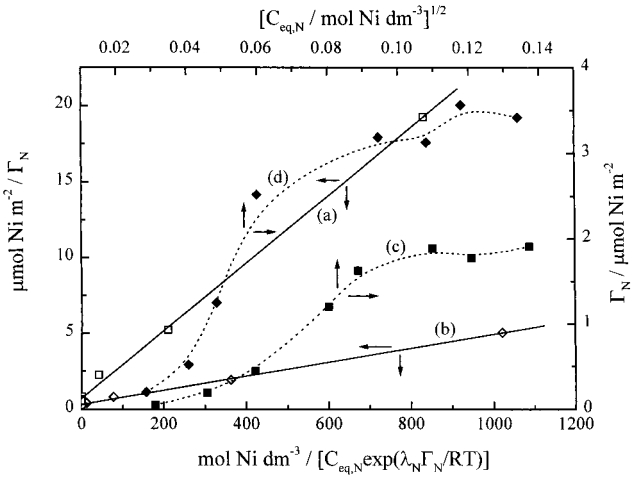

Figure 7. Plot of eqs 3 (curves c, d) and 8 (curves a, b) for the deposition of Ni^{2+} in the diffuse part of the double layer and in the IHP, respectively. The solid lines represent the values calculated using eq 8. (a) and (c) pH = 5.1, (b) and (d) pH = 6.2. $T = 25$ °C, $I = 0.15$ mol L^{-1} NH_4NO_3.

where ϵ, ϵ_0, k, N, and y_d are, respectively, the relative dielectric permittivity, the vacuum permittivity (equal to 8.854×10^{-12} C V^{-1} m^{-1}), the Boltzmann constant, the Avogadro number, and the Volta potential in the outer Helmholtz plane (OHP). A linear dependence of Γ_N on $C_{eq,N}^{1/2}$ may be anticipated according to eq 3. As may be seen in Figure 7 (dashed curves c and d), typical sets of data failed to yield a satisfactory fit according to eq 3, thus precluding the location of Ni^{2+} ions in the diffuse part of the electrical double layer of the γ-alumina/electrolyte interface. Assuming the triple-layer model and since both the surface and the diffuse part of the electrical double layer are excluded as possible sites for the location of the deposited Ni(II) ions, they should be located at the IHP.

From the above considerations it may be concluded that the preparation of WO_3-NiO/γ-Al_2O_3 catalysts with co-deposition of W(VI) species and Ni(II) ions using the EDF method results in higher amounts of supported-phase WO_3-NiO in comparison with the quantities obtained when W(VI) species and Ni(II) ions are separately deposited using the EDF method. Moreover, it may be concluded that the catalytic activity of the aforementioned catalysts may be increased by selecting the appropriate pH value for the impregnating solution so as to obtain supported-phase WO_3-NiO with the optimum value for the ratio between the amount of the active species and the promoter (W/Ni) (Figures 1 and 2). As already mentioned in the Introduction section, a feature which is very important for the activity of the prepared WO_3-NiO/γ-Al_2O_3 catalysts is the type of the deposited W(VI) species, i.e., monomeric or polymeric. Unfortunately, the semiquantitative approach of the phenomenon does not allow for the detailed investigation of this feature. The speciation of the deposited species is possible only by means of a detailed model, which may describe the particular role of each species.

Speciation of the Deposited Species—Co-Deposition Model. *Model Equilibria.* To develop a model describing the simultaneous deposition of the$W_xO_y^{z-}$ and Ni^{2+} ions on the γ-Al_2O_3 surface, it was tentatively assumed that the models developed for the separate deposition of the W(VI) species[46] and Ni(II) ions[33] on γ-alumina may also be used for the description of the co-deposition of these species. According to these models, the deposition of the W(VI) species on the γ-alumina surface may be described by the following equilibria

$$AlOH_2^+ + WO_4^{2-} \overset{k_{f,1}}{\leftrightarrow} AlOH_2^+\cdots WO_4^{2-} \quad (4a)$$

$$AlOH_2^+ + HW_6O_{20}(OH)_2^{5-} \overset{k_{f,2}}{\leftrightarrow} AlOH_2^+\cdots HW_6O_{20}(OH)_2^{5-} \quad (4b)$$

$$AlOH + WO_4^{2-} \overset{k_{f,3}}{\leftrightarrow} AlO(WO_2)O^- + OH^- \quad (4c)$$

$$2AlOH + WO_4^{2-} \overset{k_{f,4}}{\leftrightarrow} AlO(WO_2)OAl + 2OH^- \quad (4d)$$

and the deposition of the Ni(II) ions is described by equilibrium 5

$$AlO^- + Ni^{2+} \overset{k_{f,5}}{\leftrightarrow} AlO^-\cdots Ni^{2+} \quad (5)$$

Following the first model the WO_4^{2-} ions, located at the IHP, may be deposited either by adsorption at a site created by one protonated surface hydroxyl ($AlOH_2^+$), resulting in the adsorbed species shown in equilibrium 4a or by reaction with one or two adjacent undissociated surface hydroxyls (AlOH), resulting in the formation of the surface complexes shown in equilibria 4c and 4d. Similarly, the $HW_6O_{20}(OH)_2^{5-}$ ion, also located at the IHP, may be adsorbed at a site created by one protonated surface hydroxyl, resulting in the adsorbed species shown in equilibrium 4b. Following the second model, the deposition of the Ni^{2+} ions, which are at the IHP, takes place by adsorption at a site created by one deprotonated surface hydroxyl (AlO^-), resulting in the adsorbed species shown in equilibrium 5. The right-hand side of the aforementioned adsorbed species is located in the IHP, whereas the left-hand side of these species is located on the surface of γ-alumina.[46,33] It should be noted that according to these models lateral interactions, relatively strong in the case of W(VI) species[46] and very weak in the case of Ni^{2+} ions,[33] are exerted among the deposited WO_4^{2-}, $HW_6O_{20}(OH)_2^{5-}$, and Ni^{2+} ions, through water molecules located at the IHP.

Model Equations. A series of equations corresponding to equilibria 4 and 5 were derived, and the equilibrium concentrations of various species present either in the bulk solution or at the solid/liquid interface were calculated using the SURFEQL software. It was therefore possible to calculate the following parameters: (i) isotherms for the $W_xO_y^{z-}$ and Ni^{2+} ions' uptake, (ii) the ζ-potential, which may be considered to be equal to y_d,[55] in the presence of $W_xO_y^{z-}$ and Ni^{2+} ions, and (iii) the difference in the hydrogen ions consumed on the surface of γ-alumina, for the protonation of the deprotonated and neutral surface hydroxyls, in the presence and absence of $W_xO_y^{z-}$ and Ni^{2+} ions. Finally, the validity of the above-mentioned models (equilibria 4 and 5), in the case of the co-deposition of the W(VI) species and Ni(II) ions on the γ-alumina surface, may be tested by comparing the calculated parameters with the corresponding experimental results.

Regarding the derivation of the model equations, details have been reported earlier.[35,56] Following the procedure described in refs 35 and 56 for the $Cr_xO_y^{z-}$ and $Mo_xO_y^{z-}$ ions, respectively, the equation describing the deposition of the $W_xO_y^{z-}$ ions is

$$\frac{1}{\Gamma_W} = \frac{1}{\Gamma_{W,m}} + \frac{1}{\Gamma_{W,m}\tilde{K}C_{eq,W}\exp(E_W\Gamma_W/\Gamma_{W,m}RT)} \quad (6)$$

where E_W is the energy of the lateral interactions among the deposited $W_xO_y^{z-}$ ions. The constant $\tilde{K}$ is given by

$$\tilde{K} = (a_1 + a_2)K_a + a_1K_b10^{14-pH} + a_1K_b^2 10^{28-2pH} \quad (7)$$

TABLE 1: Parameters Used for the Application of SURFEQL Calculations to the Proposed Model

parameter	symbol	value	units	ref
total surface sites density	N_s	8	sites nm^{-2}	57, 58
deprotonation constant of $AlOH_2^+$	K_1^{int}	$10^{-3.87}$		35
deprotonation constant of AlOH	K_2^{int}	$10^{-7.41}$		35
W(VI) deposition constant	K			eq 6
constant of W deposition through electrostatic forces	K_a			guess (see refs 34, 35)
constant of W deposition through chemical reaction	K_b			determined from eq 7
constant of Ni deposition	K_N			eq 8
ratio of WO_4^{2-} ($HW_6O_{20}(OH)_2^{5-}$) ions concentration to the total W^{VI} concentration in the bulk solution	a_1 (a_2)			47
energies of the lateral interactions	$E_{W,a}$ $E_{N,a}$		kJ mol^{-1}	31, 32
	E_W, E_N		kJ mol^{-1}	eqs 6, 8
total W^{VI} concentration	$[W^{VI}]_t$		mol dm^{-3}	experimental
total NH_4^+ (NO_3^-) concentration	$[NH_4^+]_t$($[NO_3^-]_t$)		mol dm^{-3}	experimental
total Ni^{2+} concentration	$[Ni^{2+}]_t$		mol dm^{-3}	experimental
pH	pH			experimental
specific surface area	S.S.A.	123	m^2 g^{-1}	experimental
solid concentration	S.C.	3.57	g dm^{-3}	experimental
ionic strength	I	0.15	mol dm^{-3}	experimental
inner capacitance	C_1	9.9	F m^{-2}	
outer capacitance	C_2	0.2	F m^{-2}	

where a_1 and a_2 are the proportionality coefficients between the equilibrium concentration of the WO_4^{2-} and $HW_6O_{20}(OH)_2^{5-}$ ions in the bulk solution, respectively, and the total equilibrium concentration of the W(VI) species. These coefficients may be calculated at any pH value on the basis of the solution equilibria[47] using the SURFEQL software. Constant K_a corresponds to the deposition of the W(VI) species according to equilibria 4a and 4b, and K_b corresponds to the deposition of the W(VI) species according to equilibria 4c and 4d.

The model equation describing the deposition of Ni(II) ions may be derived following the same procedure as that in refs 33 and 56 for Co(II) ions

$$\frac{1}{\Gamma_N} = \frac{1}{\Gamma_{N,m}} + \frac{1}{\Gamma_{N,m} K_N C_{eq,N} \exp(E_N \Gamma_N / \Gamma_{N,m} RT)} \qquad (8)$$

where E_N is the energy of lateral interactions among the adsorbed Ni^{2+} ions. The constant K_N is given by the equation

$$K_N = \exp[(-\Delta G^\circ_{cs,N} - 2Fy_{IHP} - F\varphi_0)/RT] \qquad (9)$$

where $\Delta G^\circ_{CS,N}$ represents the contribution of the chemical interactions between the absorbed Ni^{2+} ions and the γ-alumina surface to the standard free energy of adsorption due to the total chemical interactions, $\Delta G^\circ_{chem,N}$, corresponding to equilibrium 5. ϕ_0 and y_{IHP} represent the Galvani potential on the surface and the Volta potential in the IHP, respectively.

Finally, the formation constants of the surface complexes illustrated on the right-hand side of equilibria 4 and 5, $K_{f,i}$ (i = 1−5) may now be calculated by the following equations:

$$K_{f,i} = K_a \exp(E_W \Gamma_W / \Gamma_{W,m} RT), \quad i = 1, 2 \qquad (10)$$

$$K_{f,3} = K_b \exp(E_W \Gamma_W / \Gamma_{W,m} RT) \qquad (11)$$

$$K_{f,4} = K_b^{\,2} \exp(E_W \Gamma_W / \Gamma_{W,m} RT) \qquad (12)$$

$$K_{f,5} = K_N \exp(E_N \Gamma_N / \Gamma_{N,m} RT) \qquad (13)$$

Test of the Postulated Model. Plot of the experimental deposition data according to eqs 6 and 8, that is $1/\Gamma_W$ vs $1/C_{eq,W} \exp(\lambda_W \Gamma_W/RT)$ and $1/\Gamma_N$ vs $1/C_{eq,N} \exp(\lambda_N \Gamma_N/RT)$, where the parameters λ_W and λ_N are equal to $E_W/\Gamma_{W,m}$ and $E_N/\Gamma_{N,m}$, respectively, allows for the determination of the values of $\Gamma_{W,m}$, $\tilde{K}$, E_W and $\Gamma_{N,m}$, K_N, E_N. These plots are expected to be linear

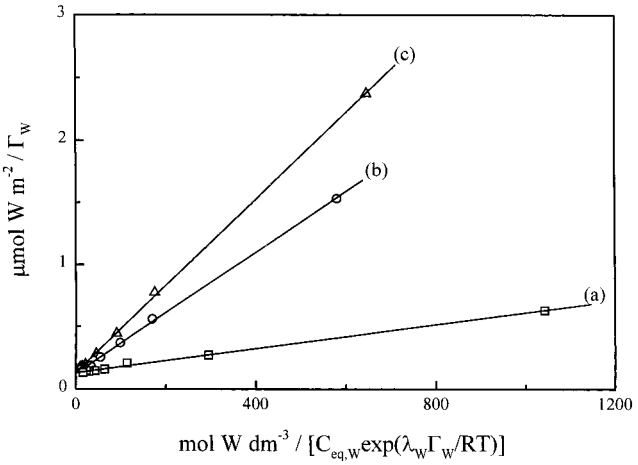

Figure 8. Plot of the reciprocal surface concentration of W(VI) as a function of $1/C_{eq,W} \exp(\lambda_W \Gamma_W/RT)$. The solid lines represent the values calculated using eq 6. (a) pH = 5.1, (b) pH = 5.7, (c) pH = 6.2. T = 25 °C, I = 0.15 mol L^{-1} NH_4NO_3.

for the appropriate λ_W and λ_N values. Typical examples are shown in Figures 7 (curves a and b) and 8. The application of the computer program SURFEQL in our system, through inserting the parameters compiled in Table 1, makes it possible for the calculation of the parameters illustrated in Table 2. These calculations allow for the construction of the deposition isotherms of the $W_xO_y^{z-}$ ions (Ni^{2+} ions), plotting the calculated equilibrium concentration of the deposited W(VI) species (Ni^{2+} ions) vs the calculated equilibrium concentration of the W(VI) species (Ni^{2+} ions) in the bulk solution, for a selected pair of K_a and K_b values which are fitted to eq 7. The validity of the selected values for K_a and K_b may then be tested by comparison of the calculated values with the experimental deposition isotherms.

Satisfactory agreement was obtained for the W(VI) deposition isotherms, at all pH values studied, for a pair of K_a and K_b values selected at each pH under the following conditions: (i) The energy of the lateral interactions exerted between one adsorbed WO_4^{2-} ion (surface complex of equilibrium 4a) or one adsorbed $HW_6O_{20}(OH)_2^{5-}$ ion (surface complex of equilibrium 4b) and the ions deposited in their vicinity is two or five times, respectively, the energy of interactions exerted between one WO_4^{2-} ion deposited according to equilibrium 4c and the ions deposited in its vicinity. (This assumption is reasonable

TABLE 2: Parameters or Variables Derived from the Application of SURFEQL to the Proposed Model

parameter	symbol	units
surface charge density	σ_o	C m^{-2}
charge density at the IHP	σ_1	C m^{-2}
charge density at the OHP	σ_d	C m^{-2}
surface potential	y_0	V
potential at the IHP	y_1	V
potential at the OHP	y_d	V
equilibrium concentration of H^+	$[H_b^+]$	mol dm^{-3}
equilibrium concentration of W^{VI} species in the bulk solution	$[H_xW_yO_z(OH)_m^{n-}]_b$	mol dm^{-3}
equilibrium concentration of Ni^{2+}	$[Ni^{2+}]_b$	mol dm^{-3}
equilibrium concentration of NH_4^+	$[NH_4^+]_b$	mol dm^{-3}
equilibrium concentration of NO_3^-	$[NO_3^-]_b$	mol dm^{-3}
equilibrium concentration of $AlOH_2{+}\cdots WO_4^{2-}$	$[AlOH_2^+\cdots WO_4^{2-}]$	mol dm^{-3}
equilibrium concentration of $AlOH_2^+\cdots HW_6O_{20}(OH)_2^{5-}$	$[AlOH_2^+\cdots HW_6O_{20}(OH)_2^{5-}$	mol dm^{-3}
equilibrium concentration of $AlO(WO_2)O^-$	$[AlO(WO_2)O^-]$	mol dm^{-3}
equilibrium concentration of $AlO(WO_2)OAl$	$[AlO(WO_2)OAl]$	mol dm^{-3}
equilibrium concentration of $AlO^-\cdots Co^{2+}$	$[AlO^-\cdots Co^{2+}]$	mol dm^{-3}
equilibrium concentration of AlOH	[AlOH]	mol dm^{-3}
equilibrium concentration of $AlOH_2^+$	$[AlOH_2^+]$	mol dm^{-3}
equilibrium concentration of AlO^-	$[AlO^-]$	mol dm^{-3}

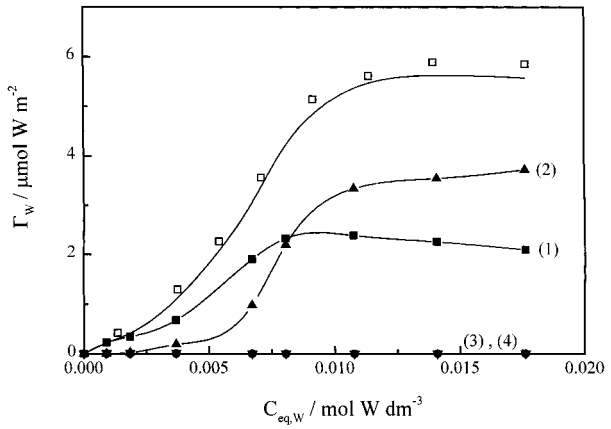

Figure 9. Variation of the surface concentration of W(VI) with the equilibrium W(VI) concentration: experimental (□) and calculated (solid lines) isotherm for the total W(VI) deposition. Calculated isotherms for the W(VI) deposition through adsorption of one WO_4^{2-} ion per site created by one $AlOH_2^+$ group (1), of one $HW_6O_{20}^{5-}$ ion per site created by one $AlOH_2^+$ group (2), and through reaction of one WO_4^{2-} ion with one (3) or two adjacent (4) AlOH groups. pH = 6.2. T = 25 °C, I = 0.15 mol L^{-1} NH_4NO_3.

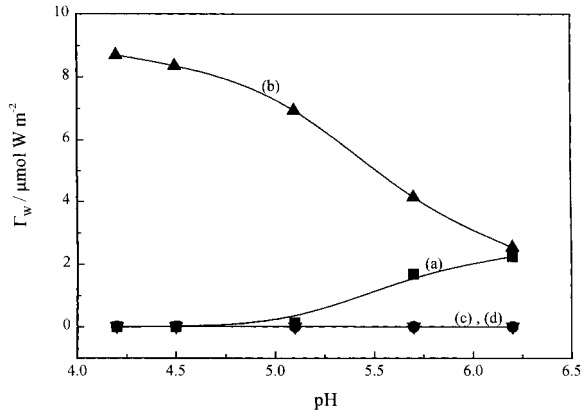

Figure 10. Variation, with pH, of the maximum amount of W deposited through adsorption of the WO_4^{2-} (curve a) and $HW_6O_{20}(OH)_2^{5-}$ (curve b) ions on sites created by the $AlOH_2^+$ groups and through reaction of one WO_4^{2-} ion with one or two adjacent surface hydroxyls (curves c, d).

considering the electric charge of the surface complexes and the fact that the lateral interactions are mainly electrostatic.) (ii) The lateral interactions are exerted mainly among the electrically charged surface complexes, formed according to equilibria 4a−4c, through water molecules and/or through water molecules and Ni^{2+} ions located in the IHP. (iii) The energy of the lateral interactions determined, E_W, is given by eq 14

$$E_W = \frac{E_{W,a} + E_{W,p}}{2} \tag{14}$$

where $E_{W,a}$ and $E_{W,p}$ represent, respectively, the energy of the lateral interactions exerted between the deposited W(VI) species separated exclusively by water molecules[32,46] and that of those separated by water molecules and Ni^{2+} ions. (iv) At all pH values studied, the lateral interactions are exerted among the deposited W(VI) species through water molecules and Ni^{2+} ions. This means that the negatively charged surface complexes illustrated in equilibria 4a−4c are shielded by the positively charged surface complexes illustrated in equilibrium 5.

Figure 9 shows a typical deposition isotherm for the W(VI) species obtained experimentally (□) and the corresponding isotherm calculated by applying SURFEQL to the postulated model (solid line). In the same plot, the isotherms calculated for the W(VI) deposition through adsorption of one WO_4^{2-} ion (1) or one $HW_6O_{20}(OH)_2^{5-}$ ion (2) per site created by one $AlOH_2^+$ group and through reaction of one WO_4^{2-} ion with one (3) or two (4) AlOH groups are shown. It should be noted that excellent agreement between experimental and predicted isotherms was obtained at all pH values investigated. There is only one pair of (K_a, K_b) values for which agreement between the theoretical and experimental isotherms was obtained. These values depended strongly on the postulated deposition mechanism, and consequently, on the analytical form of the function $\tilde{K} = f(K_a, K_b)$. Change of the assumed uptake mechanism and, thus, of the analytical form of the aforementioned function, failed to lead to sets of adsorption constants such that agreement between the calculated and experimental curve could be obtained.

Plots of the maximum amount of the W(VI) species deposited according to equilibria 4a−4d, which corresponds to the plateau of the respective calculated deposition isotherm (such as those illustrated in Figure 9), versus pH are shown in Figure 10. In Figure 10, the variation of the saturation surface concentration of W(VI) deposited according to equilibrium 4a (curve a), 4b (curve b), 4c (curve c), and 4d (curve d) as a function of the solution pH is shown. The negligible deposition of W(VI) according to equilibria 4c and 4d (see isotherms 3 and 4 in Figure 9 and curves c and d of Figure 10) demonstrates that

the presence of Ni(II) ions in the impregnating solution minimized the contribution of the undissociated surface hydroxyls to the total W(VI) uptake. The negligible deposition through chemical reaction with the neutral surface hydroxyls may be explained mathematically on the basis of the aforementioned conditions, under which a satisfactory agreement was obtained between the calculated and experimental W(VI) uptake isotherms. According to these conditions, relatively high values for the adsorption constants $K_{f,1}$ and $K_{f,2}$ (eq 10) and relatively low values for the reaction constants $K_{f,3}$ and $K_{f,4}$ (eqs 11 and 12) are computed. The relatively high values of $K_{f,1}$ and $K_{f,2}$ lead, on one hand, to enhanced amounts of W(VI) species deposited by adsorption (equilibria 4a,b) and, on the other hand, to negligible deposition taking place through reaction (equilibria 4c,d) (Figures 9 and 10). Moreover, curve a (curve b) of Figure 10 shows an increase (decrease) of the maximum amount of W deposited through adsorption of the WO_4^{2-} [$HW_6O_{20}(OH)_2^{5-}$] ions, with pH. These trends show that it is possible to regulate the ratio "monomeric/polymeric deposited W(VI) species" by changing the pH of the impregnating solution. The value of this ratio strongly affects the catalytic activity of the prepared W−Ni/γ-alumina catalyst.

For the Ni(II) uptake on γ-alumina, satisfactory agreement between calculated (solid lines in Figure 2) and experimental isotherms was obtained all pH values studied under the following conditions: (i) The determined energy of the lateral interactions is given by eq 15

$$E_N = \frac{E_{N,a} + E_{N,p}}{2} \qquad (15)$$

where $E_{N,a}$ and $E_{N,p}$ represent the energy of the lateral interactions exerted between the adsorbed Ni^{2+} ions exclusively through water molecules[31,33] and through water molecules and $W_xO_y^{z-}$ ions. (ii) The term $\Delta G^\circ_{cc,N}$, which represents the contribution to the total free energy of adsorption, $\Delta G^\circ_{ads,N}$, of the interactions (chemical and electrostatic) exerted among the adsorbed Ni^{2+} ions, should be expressed by eq 16

$$\Delta G^\circ_{cc,N} = -0.2[E_{N,p}(1 - \theta_N) + E_N\theta_N] \qquad (16)$$

instead of $-E_N\theta_N$[59] stated for the derivation of eq 8. The assumption underlying eq 16 may be justified as follows: For relatively small θ_N values (first points of the deposition isotherms), the probability of lateral interactions exerted between the deposited Ni^{2+} ions shielded by $W_xO_y^{z-}$ ions and water molecules is relatively high (the first term of the right-hand side of eq 16 becomes important). On the contrary when θ_N is relatively large (points toward the plateau region of the deposition isotherms), the lateral interactions are exerted between ions separated either by water molecules or by water molecules and $W_xO_y^{z-}$ ions (the second term of the rhs of eq 16 becomes important). The above assumption may be tested by means of eq 8, which in view of the above (eq 16), is transformed into eq 17

$$\frac{1}{\Gamma_N} = \frac{1}{\Gamma_{N,m}} + \frac{1}{\Gamma_{N,m}K_N C_{eq,N} \exp\{0.2[E_{N,p}(1 - \theta_N) + E_N\theta_N]/RT\}} \qquad (17)$$

According to eq 17 a linear variation of $1/\Gamma_N$ with $1/C_{eq,N}$ $\exp\{0.2[E_{N,p}(1 - \theta_N) + E_N\theta_N]/RT\}$ is predicted. Typical examples, showing the excellent fit of the experimental data to the model (eq 17), are presented in Figure 11.

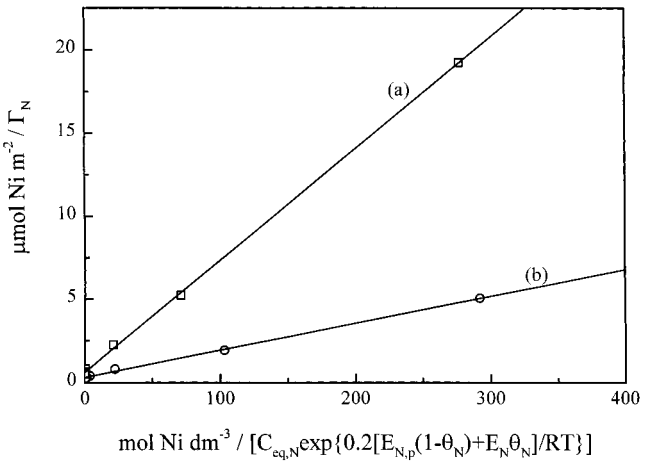

Figure 11. Plot of eq 17. The solid lines represent the values calculated using eq 17. (a) pH = 5.1 and (b) pH = 6.2. T = 25 °C, I = 0.15 mol L^{-1} NH_4NO_3.

TABLE 3: Values of the Energy of the Lateral Interactions Corresponding to W(VI) and [Ni(II)] Deposition in the Absence (Columns a) and Presence (Columns b) of Ni(II) Ions [W(VI) Species], as Well as Values of the Deposition Constant Corresponding to Ni(II) Deposition in the Absence (Column a) and Presence (Column b) of W(VI) at Different pH Values

			E (KJ mol^{-1})			
	K_N		W(VI)		Ni(II)	
pH	*a*	*b*	*a* ($E_{w,a}$)	*b* (E_w)	*a* ($E_{N,a}$) × 10^2	*b* (E_N)
4.2	316.0[a]	19.92	−0.72[b]	6.52	0.0[a]	18.13
4.5	384.0[a]	24.35	−0.90[b]	4.26	0.0[a]	12.56
5.1	310.0	31.36	6.83[b]	6.91	2.1	15.26
5.7	288.0[a]	19.67	0.12	7.98	2.9[a]	24.89
6.2	408.0[a]	68.86	4.15[b]	6.95	6.5[a]	7.92

[a] Reference 31. [b] Reference 32.

Table 3 compiles the values of the energy of the lateral interactions, E_W and E_N, determined from eqs 6 and 8, respectively, and the values of the deposition constant, K_N, determined from eq 8. Columns a and b correspond to the separate deposition of W(VI) species and Ni(II) ions and to their co-deposition. A considerable increase in the energy of the lateral interactions exerted between the deposited W(VI) species and Ni(II) ions resulting from the presence of Ni^{2+} and $W_xO_y^{z-}$ ions, respectively, may be observed at almost all pH values investigated, thus corroborating the qualitative conclusion that stronger attractions are exerted between the simultaneously deposited $W_xO_y^{z-}$ and Ni^{2+} ions in comparison with the case in which the $W_xO_y^{z-}$ and Ni^{2+} ions are deposited separately.

Provided that the deposition constant, K_N, is a function of the interactions (chemical and electrical) between the deposited species and the substrate[60] (eq 9), the reduced values of K_N (Table 3) imply that the strength of interactions of the adsorbed Ni^{2+} ions with γ-alumina is lower in the presence than in the absence of W(VI) species. Therefore, the increased attractive lateral interactions in combination with the lower strength of the Ni···Al_2O_3 interactions are expected to inhibit the formation of the catalytically inactive $NiAl_2O_4$, when a WO_3−NiO/γ-Al_2O_3 catalyst is prepared by depositing, simultaneously, both W(VI) species and Ni(II) ions using the EDF method.

Additional support for the proposed model was obtained from measurements of electrophoretic mobilty of γ-alumina particles in the presence of W(VI) species and Ni(II) ions. As may be seen in Figure 6, excellent agreement was obtained between the experimentally determined data and the prediction according

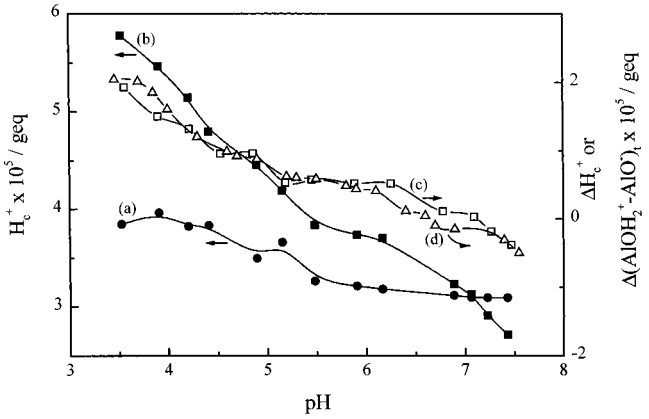

Figure 12. Variation with pH of: (i) Hydrogen ions consumed on the surface, H_c^+, in the absence (curve a) and in the presence (curve b) of $W_xO_y^{z-}$ (1×10^{-3} mol $W^{(VI)}$ L^{-1}) and Ni^{2+} (1×10^{-3} mol Ni^{2+} L^{-1}) ions, (ii) the differences (in the presence and absence of $W_xO_y^{z-}$ and Ni^{2+} ions) in the hydrogen ions consumed on the surface, ΔH_c^+, (curve c) as well as of the "total protonated minus total deprotonated surface hydroxyls", $\Delta(AlOH_2^+ - AlO^-)_t$ (curve d). ΔH_c^+ was determined experimentally whereas $\Delta(AlOH_2^+ - AlO^-)_t$ was calculated using the proposed model. $T = 25$ °C, $I = 0.15$ mol L^{-1} NH_4NO_3.

to the proposed model, using SURFEQL for the calculation of the value of the ζ-potential.

Finally, the variation with pH of the protons consumed on the surface of γ-alumina, H_c^+, in the absence (curve a) and in the presence (curve b) of $W_xO_y^{z-}$ and Ni^{2+} ions is illustrated in Figure 12. Curves a and b were obtained by subtracting the potentiometric titration curves corresponding to the electrolyte solutions (blank titrations) from the respective curves of the suspensions. Details concerning calculations on titration curves are given in refs 35, 56, and 59. The higher values of H_c^+ obtained in the presence of W(VI) species and Ni(II) ions (curve b), where the adsorbed, negatively charged $W_xO_y^{z-}$ ions are significantly more than the adsorbed positively charged Ni^{2+} ions (cf. Figures 1 and 2), are in agreement with the well-known feature of the double layer: the proton uptake on the surface increases upon specific adsorption of anionic species. By subtracting curve a from curve b of Figure 12, the difference in the protons consumed on the surface of γ-alumina in the presence and in the absence of $W_xO_y^{z-}$ and Ni^{2+} ions, ΔH_c^+, may be determined (Figure 12, curve c). Moreover, Figure 12 (curve d) shows the variation with pH of the difference of the "total protonated minus total deprotonated surface hydroxyls" in the presence and absence of $W_xO_y^{z-}$ and Ni^{2+} ions, $\Delta(AlOH_2^+ - AlO^-)_t$, calculated from the variables compiled in Table 2, which were derived from the application of SURFEQL to the proposed model. The excellent agreement obtained between the variation of ΔH_c^+ (Figure 12, curve c) and $\Delta(AlOH_2^+ - AlO^-)_t$ (Figure 12, curve d) with pH, suggests that H_c^+ refers to protons consumed exclusively on the surface of γ-alumina for the protonation of the deprotonated and neutral surface hydroxyls. In other words, the amount of protons or hydroxyl ions presumably taken up by the adsorbed W(VI) and Ni(II) species seems to be similar to the amount of protons or hydroxyl ions participating in the hydrolysis equilibria of these species in solution. As a result, these protons or hydroxyl ions are eliminated when the potentiometric titration curve corresponding to the electrolyte is subtracted from the respective titration curve of the suspension.

According to the above considerations, the co-deposition of the $W_xO_y^{z-}$ and Ni^{2+} ions on the γ-alumina surface may be schematized (Figure 13).

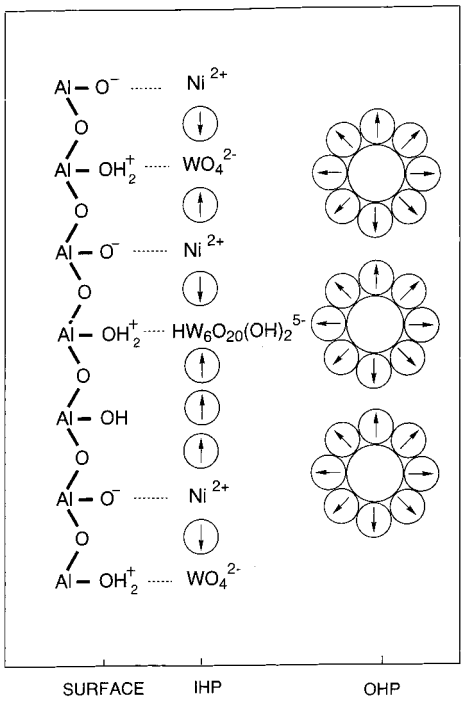

Figure 13. Schematic representation of the model for the co-deposition of WO_4^{2-}, $HW_6O_{20}^{5-}$, and Ni^{2+} ions on the γ-alumina surface.

Finally, it should be noted that any aluminum heteropolytungstate species was not taken into account due to lack of relevant data, contrary to the aluminum heteropolymolybdate (Anderson type) species often mentioned in the literature (e.g., refs 61−63).

Conclusions

The most important findings of the present work may be summarized as follows:

(i) The deposition of W(VI) species or Ni(II) ions on the γ-alumina surface, in the presence of Ni(II) ions or W(VI) species, respectively, in the impregnating solution, takes place mainly through adsorption of $W_xO_y^{z-}$ or Ni^{2+} ions on energetically equivalent sites at the IHP, with strong attractive lateral interactions among the adsorbed ions.

(ii) The protonated or deprotonated surface hydroxyls are mainly responsible for the adsorption of the $W_xO_y^{z-}$ or Ni^{2+} ions, respectively, thus resulting in a decrease (increase) in the adsorbed amount of W(VI) species (Ni(II) ions) with increasing pH.

(iii) A mutual promotion of the adsorption for the $W_xO_y^{z-}$ and Ni^{2+} ions is caused by the coadsorbed Ni^{2+} and $W_xO_y^{z-}$ ions, respectively, as a result of the stronger attractive lateral interactions exerted among the adsorbed ions, in the presence of both W(VI) species and Ni(II) ions in the impregnating solution.

(iv) The stronger lateral attractions in conjunction with the lower strength of the Ni···Al_2O_3 interactions inferred, in this study, is expected to inhibit the formation of the catalytically inactive $NiAl_2O_4$ when a WO_3−NiO/γ-Al_2O_3 catalyst is prepared by co-deposition of W(VI) and Ni(II) species following EDF.

(v) The species of W(VI) which are mainly adsorbed on the γ-alumina surface in the presence of Ni(II) ions, in the pH range 4.2−6.2, are the WO_4^{2-} and $HW_6O_{20}(OH)_2^{5-}$ ions. As pH increased from 4.2 to 6.2, the deposition of W(VI) through adsorption of WO_4^{2-} ions increased at the expense of deposition

of W(VI) through adsorption of $HW_6O_{20}(OH)_2^{5-}$ ions, which decreased. The participation of the neutral surface hydroxyls in the deposition of W(VI) species in the presence of Ni(II) ions is negligible.

(vi) The catalytic activity of the $WO_3-NiO/\gamma-Al_2O_3$ catalysts, prepared with co-deposition of W(VI) species and Ni(II) ions using the EDF method, may be maximized by selecting the appropriate pH value of the impregnating solution so as to obtain supported-phase WO_3-NiO with the optimum values for the ratios "W/Ni" and "monomeric/polymeric" W(VI) species.

(vii) The mutual promotion in the deposition of two catalytically active species with opposite charge during their co-deposition using the EDF method may be applied to the preparation and development of supported catalysts with high dispersion of the supported phase and with the desired ratio between the amount of the active species and the promoter.

Acknowledgment. Experimental facilities made available by Professor P. G. Koutsoukos and useful discussions he participated in with us throughout this study are gratefully acknowledged.

References and Notes

(1) Wang, L.; Hall, W. K. *J. Catal.* **1982**, *77*, 232.
(2) Wang, L.; Hall, W. K. *J. Catal.* **1983**, *83*, 242.
(3) Wang, L.; Hall, W. K. *J. Catal.* **1980**, *66*, 251.
(4) Kasztelan, S.; Grimblot, J.; Bonnelle, J. P.; Payen, E.; Toulhoat, H.; Jacquin, Y. *Appl. Catal.* **1983**, *7*, 91.
(5) Iannibello, A.; Marengo, S.; Trifiro, F.; Villa, P. L. In *2nd International Symposium on Scientific Bases for the Preparation of Heterogeneous Catalysts*, Louvain La Neuve, Belgium, 1978; Paper A5.
(6) Caceres, C. V.; Fierro, J. L. G.; Agudo, A. L.; Blanco, M. N.; Thomas, H. J. *J. Catal.* **1985**, *95*, 501.
(7) van Veen, J. A. R.; De Wit, H.; Emeis, C. A.; Hendriks, P. A. J. M. *J. Catal.* **1987**, *107*, 579.
(8) Milova, L. P.; Zaidman, N. M.; Plyasova, L. M.; Ketchik, S. V.; Rikhter, K. G. *Kinet. Katal.* **1982**, *23*, 123.
(9) Fiedor, J. N.; Proctor, A.; Houalla, M.; Sherwood, P. M. A.; Mulcahy, F. M.; Hercules, D. M. *J. Phys. Chem.* **1992**, *96*, 10967.
(10) Fay, M. J.; Proctor, A.; Hoffman, D. P.; Houalla, M.; Hercules, D. M. *Mikrochim. Acta* **1992**, *109*, 281.
(11) Sonnemans, J.; Mars, P. *J. Catal.* **1973**, *31*, 209.
(12) Williams, C. C.; Ekerdt, J. G.; Jehng, J. M.; Hardcastle, F. D.; Wachs, I. E. *J. Phys. Chem.* **1991**, *95*, 8791.
(13) Machej T.; Haber, J.; Turek, A. M.; Wachs, I. E. *Appl. Catal.* **1991**, *70*, 115.
(14) Wang, L.; Hall, W. K. *J. Catal.* **1983**, *82*, 177.
(15) van Veen, J. A. R.; Hendriks, P. A. J. M. *Polyhedron* **1986**, *5*, 75.
(16) Brunelle, J. P. *Pure Appl. Chem.* **1978**, *50*, 1211.
(17) Ng, K. Y. S.; Gulari, E. *J. Catal.* **1985**, *92*, 340.
(18) Contescu, Cr.; Vass, M. I. *Appl. Catal.* **1987**, 33, 259.
(19) Kim, D. S.; Kurusu, Y.; Wachs, I. E.; Hardaste, F. D.; Segawa, K. *J. Catal.* **1989**, *120*, 325.
(20) Vermaire, D. C.; van Berge, P. C. *J. Catal.* **1989**, *116*, 309.
(21) Tewari, P. H.; Lee, W. *J. Colloid Interface Sci.* **1975**, *52*, 77.
(22) Mulcahy, F. M.; Fay, M. G.; Proctor, A.; Houalla, M.; Hercules, D. M. *J. Catal.* **1990**, *124*, 231.
(23) Iannibello, A.; Mitchell, P. C. H. In *2nt International Symposium on Scientific Bases for the Preparation of Heterogeneous Catalysts*, Louvain La Neuve, Belgium, 1978; Paper E2.
(24) Baumgarten, E.; Kirchhausen-Dusing, U. *J. Colloid Interface Sci.* **1997**, *194*, 1.
(25) Hohl, H.; Stumm, W. *J. Colloid Interface Sci.* **1976**, *55*, 281.
(26) Davis, J. A.; Leckie, J. O. *J. Colloid Interface Sci.* **1978**, *67*, 90.
(27) Spanos, N.; Vordonis, L.; Kordulis, Ch.; Lycourghiotis, A. *J. Catal.* **1990**, *124*, 301.
(28) Spanos, N.; Vordonis, L.; Kordulis, Ch.; Koutsoukos, P. G.; Lycourghiotis, A. *J. Catal.* **1990**, *124*, 315.
(29) Vordonis, L.; Koutsoukos, P. G.; Lycourghiotis, A. *Colloids Surf.* **1990**, *50*, 353.
(30) Spanos, N.; Matralis, H. K.; Kordulis, Ch.; Lycourghiotis, A. *J. Catal.* **1992**, *136*, 432.
(31) Vordonis, L.; Spanos, N.; Koutsoukos, P. G.; Lycourghiotis, A. *Langmuir* **1992**, *8*, 1736.
(32) Karakonstantis, L.; Kordulis, Ch.; Lycourghiotis, A. *Langmuir* **1992**, *8*, 1318.
(33) Spanos, N.; Lycourghiotis, A. *J. Chem. Soc., Faraday Trans.* **1993**, *89*, 4101.
(34) Spanos, N.; Lycourghiotis, A. *J. Catal.* **1994**, *147*, 57.
(35) Spanos, N.; Slavov, S.; Kordulis, Ch.; Lycourghiotis, A. *Langmuir* **1994**, *10*, 3134.
(36) Vordonis, L.; Koutsoukos, P. G.; Lycourghiotis, A. *J. Chem. Soc., Chem. Commun.* **1984**, 1309.
(37) Vordonis, L.; Koutsoukos, P. G.; Lycourghiotis, A. *J. Catal.* **1986**, *98*, 296.
(38) Vordonis, L.; Koutsoukos, P. G.; Lycourghiotis, A. *J. Catal.* **1986**, *101*, 186.
(39) Akratopulu, K.; Vordonis, L.; Lycourghiotis, A. *J. Chem. Soc., Faraday Trans.* **1986**, *82*, 3697.
(40) Vordonis, L.; Koutsoukos, P. G.; Lycourghiotis, A. *Langmuir* **1986**, *2*, 281.
(41) Akratopulu, K.; Kordulis, Ch.; Lycourghiotis, A. *J. Chem. Soc., Faraday Trans.* **1990**, *86*, 3437.
(42) Koutsoukos, P. G.; Lycourghiotis, A. *Colloids Surf.* **1991**, *55*, 297.
(43) Le Page, J. F. *Catalyse de Contact*; Techinip.: Paris, 1978; p 441.
(44) Salvati, L., Jr.; Makovsky, L. E.; Stencel, J. M.; Brown, F. R.; Hercules, D. M. *J. Phys. Chem.* **1981**, *85*, 3700.
(45) Brady, R. L.; Southmayd, D.; Contescu, Cr.; Zhang, R.; Schwarz, J. A. *J. Catal.* **1991**, *129*, 195.
(46) Karakonstantis, L.; Bourikas, K.; Lycourghiotis, A. *J. Catal.* **1996**, *162*, 295.
(47) Smith, R. M.; Martell, A. E. In *Critical Stability Constants*; Plenum Publishing: New York, 1981; Vol. 4.
(48) d'Espinose de la Caillerie, J. B.; Kermarec, M.; Clause, O. *J. Am. Chem. Soc.* **1995**, *117*, 11471.
(49) Marczenko, Z. In *Spectrophotometric Determination of Elements*; Ransay, C. G., Translation Ed.; John Wiley and Sons: New York, 1970; p 569.
(50) Liberman, A. *Analyst (Cambridge, U.K.)* **1955**, *80*, 595.
(51) Giles, C. H.; D'Silva, A. P.; Easton, I. A. *J. Colloid Interface Sci.* **1974**, *47*, 766.
(52) Giles, C. H.; Smith, D.; Huitson, A. *J. Colloid Interface Sci.* **1974**, *47*, 755.
(53) Faughnan, J. *SURFEQL An Interactive Code for the Calculation of Chemical Equilibria in Aqueous Systems*; W. M. Keck Laboratories, California Institute of Technolog: Pasadena, CA 91125; pp 138−178.
(54) Bockris, J. O'M.; Reddy, A. K. N. *Modern Electrochemistry*; Plenum Press: N. Y., 1976; Vol. 2, Chapter 7.
(55) Lyklema, J. *Fundamentals of Interface and Colloid Science*; Academic Press: London, 1995; Vol. II, Chapter 4.
(56) Spanos, N.; Lycourphiotis, A. *Langmuir* **1994**, *10*, 2351.
(57) Sprycha, R. *J. Colloid Interface Sci.* **1983**, *96*, 551.
(58) Huang, C. P. *The Chemistry of the Aluminum Oxide−Electrolyte Interface*, Ph.D. Thesis, Harvard University, Cambridge, MA, 1971.
(59) Spanos, N.; Lycourghiotis, A. *J. Colloid Interface Sci.* **1995**, *171*, 306.
(60) Hough, D. B.; Rendall, H. M. In *Adsorption from Solution at the Solid/Liquid Interface*; Parfitt, G. D., Rochester, C. H., Eds.; Academic Press: London, 1983; Chapter 6.
(61) Pope, M. T. *Heteropoly and Isopoly Oxometalates*; Springer Publishing: West Berlin and Heidelberg, Germany, 1983; p 81.
(62) Ohman, L. O. *Inorg. Chem.* **1989**, *28*, 3629.
(63) Carrier, X.; Lambert, J. F.; Che, M. *J. Am. Chem. Soc.* **1997**, *119*, 10137.